

AKOYA CULTURED PEARL FARMING IN EASTERN AUSTRALIA

Laura M. Otter, Oluwatoosin B. A. Agbaje, Le Thi-Thu Huong, Tobias Häger, and Dorrit E. Jacob

Akoya cultured pearls have been produced on the eastern shoreline of Australia since approximately 1999 using *Pinctada imbricata fucata* mollusks native to New South Wales. Unlike many of their Japanese counterparts, Australian akoya cultured pearls are harvested after 18 months of growth and marketed without any post-harvest treatments involving dyes or bleaches. This study presents the first gemological and mineralogical characterization of Australian akoya cultured pearls using Raman, photoluminescence, FTIR, and UV-Vis specular reflectance spectroscopy. Raman and FTIR spectroscopy identified the major mineral phase aragonite as well as some organic compounds. While Raman spectroscopy revealed polyene-related pigments with bands occurring at 1134 and 1532 cm^{-1} , FTIR spectroscopy showed sulfate- and polysaccharide-associated groups occurring at around 1200 and 1115 cm^{-1} , respectively. UV-Vis spectroscopy revealed broad spectral features that provide insight into the distinct bodycolors and enable discrimination from some non-akoya saltwater cultured pearls from *P. margaritifera*, *P. maxima*, and *P. mazatlanica* bivalves, while separation from other untreated akoya pearls is not possible. Production processes are examined to better understand the modern, sustainable, and environmentally friendly pearl farming operations in Australia.

The *Pinctada imbricata fucata* mollusk has long been used to produce akoya cultured pearls, dating back to the pioneering work in the early 1900s by Japanese entrepreneur Kokichi Mikimoto (Strack, 2006). This bivalve is distributed widely across Asia and also occurs on the eastern coast of Australia (Gifford et al., 2004), where it is used to produce untreated and sometimes vibrantly colored cultured pearls (figure 1). With *Pinctada imbricata fucata* populations readily available on New South Wales's Central Coast region between Sydney and the city of Lake Macquarie, a local enterprise called Broken Bay Pearls with expertise in farming of edible Sydney rock oysters (*Saccostrea glomerata*) has been culturing akoya pearls since 2003 (figure 2). The climate in New South Wales is ideally suited for pearl culturing using *Pinctada imbricata fucata*. It is located approximately the same distance from the equator as the southern Japanese pearl farms, and its very similar seasonal variations of water temperature optimize nacre quality during the cultivation process (Strack, 2006; Gilbert et al., 2017).

Australia was originally known for its large-scale production of silver- and gold-colored natural and cultured South Sea pearls from *Pinctada maxima* (Scarratt et al., 2012 and references therein), which are valued for their large sizes of up to 20 mm in di-

Figure 1. A bracelet showing naturally colored blue, cream, yellow, and silver akoya cultured pearls from Broken Bay Pearls. Photo courtesy of Broken Bay Pearls Pty Ltd.



See end of article for About the Authors and Acknowledgments.

GEMS & GEMOLOGY, Vol. 53, No. 4, pp. 423–437,

<http://dx.doi.org/10.5741/GEMS.53.4.423>

© 2017 Gemological Institute of America



Figure 2. The map of Australia (A) indicates the location of the Broken Bay Pearls farm near Woy Woy in New South Wales, on the southeastern shoreline (B). The akoya pearl farming operation near Woy Woy (C) and some of the long-line systems for juvenile *Pinctada imbricata fucata* that are held nearby (D). For scale, the wooden jetty shown in C and D is 1.5 meters wide. Photos by Laura Otter.

ameter (Strack, 2006). Australian akoya cultured pearls have yet to receive comparable attention in the gemological community. This study aims to characterize the occurrence of akoya cultured pearls in eastern Australia and presents what is believed to be the first thorough gemological and mineralogical characterization through Raman, photoluminescence (PL), ultraviolet-visible (UV-Vis), and Fourier-transform infrared (FTIR) spectroscopic analysis.

Hatchery and Spat Production. For about a decade, the hatchery facilities located at NSW Fisheries, Port Stephens Fisheries Institute (PSFI) have supplied Broken Bay Pearls with young *Pinctada imbricata fucata*. Broodstock are collected from both the farm and in the wild and selected based on nacre color and

shell shape. Priority is given to stock with more convex shells, which allow for larger nuclei to be implanted during seeding. These parents are brought to the hatchery, where spawning is induced by increasing water temperatures by about 4°C. Eggs and sperm are mixed in 1,000-liter tanks. They are kept at 24–26°C until they develop into larvae (figures 3A and 3B) after 20–24 hours; water temperature, feeding protocols, and stock density are regulated as needed (O'Connor et al., 2003). The larval cycle takes approximately three weeks before they are ready to settle from the water column and attach to a substrate such as mesh screens or bags.

After settlement, these spat are retained until reaching approximately 1.5 mm in size, whereupon they are transferred from the hatchery in Port

Stephens to the pearl farm near Woy Woy (figure 2). Here, they are placed in 0.5 mm mesh bags (figure 3C) attached to several parallel long-line systems about 200 meters in length and situated at a depth of 4 meters below the low tide water level. As the juvenile *Pinctada imbricata fucata* bivalves grow, they are progressively transferred to larger mesh bags or cages that are cleaned regularly to ensure good water flow.

Broken Bay Pearls is currently the only akoya pearl farm on the New South Wales coastline. Several small islands act as a barrier between the open ocean and the farm, creating a well-protected bay that is ideally suited for pearl farming. This area within the estuary provides stable salinity, nutrient availability, and high levels of dissolved oxygen, which are key factors for the long-term development and cultivation of a healthy stock.

Seeding and Maintaining of Australian Akoya Pearl Oysters. The juvenile pearl oysters are maintained on the farm until they are approximately two years old with shell heights of about 7 cm. Similar to other farms, the mollusks are cleaned with high-pressure cleaners every two to four weeks (Gifford et al., 2004).

It is common practice to condition the pearl oysters for several weeks before seeding by reducing their physiological fitness. At Broken Bay this is achieved by stocking the mollusks at high density within barnacle-overgrown wicker baskets that restrict water flow and food availability. Other farms, such as those in Southeast Asia, cover the mollusks with fabric to achieve the same effect (Hänni, 2007). Either way, they respond to food shortage by ceasing gamete production that would otherwise interfere with the seed-

ing process (Hänni, 2007). This conditioning strategy allows the seeders at Broken Bay Pearls to process the animals without having to apply relaxant drugs to immobilize them (Acosta-Salmón et al., 2005).

The bivalves are seeded in the austral summer month of February using only shells of suitable size (shell height larger than 7 cm) and fitness. This ensures acceptance of the bead, fast recovery from sur-

In Brief

- Gem-quality akoya bead cultured pearls have been produced on Australia's eastern shoreline since 1999, with environmentally friendly strategies to achieve sustainable farming.
- A wide variety of colors occur naturally besides the traditional white and silver. These cultured pearls are marketed without the application of bleaches or dyes.
- Australian retailers have embraced these akoya cultured pearls as locally manufactured jewelry becomes increasingly popular in the country.
- This work suggests that colored akoya cultured pearls produced by *P. imbricata fucata* can be differentiated from pearls from other species such as *P. margaritifera*, *P. maxima*, and *P. mazatlanica* using UV-Vis spectroscopy.

gery, and a greater chance for successful pearl growth. The production of cultured pearls requires two types of mollusk broodstock. Donor mollusks are selected for nacre color and quality and are sacrificed in the seeding process to extract the mantle tissue graft that is later inserted with the bead. The host animals, on



Figure 3. Australian *Pinctada imbricata fucata* larvae, shown here at an age of about 25 hours (A) with approximately 200 μm shell size, are reared in 1,000-liter polyethylene tanks at the nursery (B). After 24 days, the larvae mature to spat with approximately 1.5 mm shell lengths. They are transferred to long-line systems and kept in 0.5 mm nylon mesh bags (C). Photos by Wayne A. O'Connor.



Figure 4. These photos show the steps involved in the seeding of Australian akoya pearls. A: The outermost part of the mantle lobe is cut from a donor mollusk. B: The outer epithelial tissue is separated from the darker marginal mantle part using a scalpel. C: The outer epithelial tissue is cut into small, approximately 2 × 2 mm tissue grafts (*saibo*). D: An incision is carefully made in the gonad, while the bivalve is affixed to an oyster stand. E: The 6 mm beads are manufactured from American freshwater mussel shells. F: Tissue and bead are inserted into the gonad. Photos by Laura Otter.

the other hand, are selected for fitness and health to enable optimal proliferation of the tissue graft into a nacre-producing pearl sac (Hänni, 2012). The two Australian seeders at Broken Bay Pearls were trained by Japanese specialists who also visit regularly during harvests. Each year they insert several thousand beads—exact numbers remain confidential—together with tissue grafts. Two beads are inserted per mollusk.

Tissue grafts are prepared following the Japanese method. First, the outermost part of the mantle lobe is removed from the donor (figure 4A) and the outer epithelial tissue is carefully separated from the

darker marginal mantle tissue (figure 4B). Then the outer epithelial tissue is cut into approximately 2 × 2 mm pieces, known as the *saibo* or graft (figure 4C). The gonad in the donor mollusk is opened (figure 4D), and each tissue graft is carefully inserted into the mollusk together with a 6 mm bead manufactured from American freshwater mussel shells (figure 4E). Graft and bead are carefully placed in contact with each other (figure 4F). Since the gonad tissue itself is unable to produce pearls, the bead must be accompanied by the mantle tissue graft. Following the seeding process, the graft proliferates to form a pearl sac, fully enclosing the bead (Hänni, 2012) and pro-

TABLE 1. Characteristics of natural-color cultured pearls from *Pinctada imbricata fucata* bivalves from eastern Australia.

Photo ^a	Sample no.	Diameter (mm)	Weight (ct)	Bodycolor ^b	Hue ^b	Overtone ^b
	BBP01	7.3	3.01	Light yellow	Green	Yellow
	BBP02	6.7	2.20	Light yellow	Orange	Gold
	BBP03	7.0	2.51	Dark yellow	Orange	Green
	BBP04	6.9	2.48	Dark yellow	Orange	Gold, orange
	BBP05	6.9	2.50	Orange	Brown	Pink
	BBP06	7.5	3.03	Pinkish orange	Green	Pink
	BBP07	7.4	2.90	Silver	Blue	Blue, pink
	BBP08	6.8	2.31	White	Silver	Pink
	BBP09	7.2	2.66	White	Cream	Pink
	BBP10	7.0	2.49	Silver	Green	Blue
	BBP13	7.9	3.56	Green	Silver	Pink
	BBP14	7.7 × 8.2	3.65	Green	Silver	Blue
	BBP11 ^c	6.7	2.00	Dark blue	Green	Silver, blue
	BBP12	7.2	2.48	Silver (darker than BBP07 and BBP10)	Green	Blue, pink

^aImages not to scale. Bead sizes are 6 mm for all specimens shown.

^bBodycolor, hue, and overtone were determined by visual examination. Bodycolor descriptions follow the GIA scheme (<https://www.gia.edu/pearl-description>), but extending the scheme was necessary to incorporate the large range of color in these samples.

^cColor was found to vary from blue on one side to silver with only a blue hue and overtone on the other. All spectroscopic measurements were taken from the blue side.

ducing calcium carbonate, causing the deposition of nacre onto the bead (Jacob et al., 2011). Hence, the relative position between tissue graft and bead as well as the position within the pearl sac determine the eventual shape of the pearl: In the ideal case, when tissue graft and bead are in tight contact, a round pearl is formed. Near-round, semi-baroque, or baroque pearls are formed by an irregular contact between bead and graft that results in cavities or even loose beads (Hänni, 2012; Otter et al., 2014).

Harvesting and General Farming Procedures of Australian Akoya Cultured Pearls. After seeding, the *Pinctada* bivalves are returned to the long-line systems in bags or cages, where their food supply is no longer restricted. Their metabolic activity increases, and the production of nacre needed for shell growth and pearl development returns to normal. Hence, the bulk of pearl growth occurs during the austral summer months (December to February), when the ani-

mals have an increased metabolism and food is abundant. In contrast, a finer and therefore more lustrous outermost layer of nacre is deposited in austral winter (June to August), when colder temperatures slow down metabolic and biomineralizing processes (Gilbert et al., 2017).

Bead rejection rates are approximately 10%, which is relatively low compared to farms in the Federated States of Micronesia (28%) or southwest India (14%), while recent rejection rates from Japan were not available in the literature (Kripa et al., 2007 and references therein; Cartier et al., 2012). Broken Bay Pearls generally allows a longer cultivation time of 18 months to achieve a thicker nacre, compared to the standard 6–12 months in Japan (Strack, 2006). The longer cultivation time results in a nacre layer around the bead measuring approximately 0.8 mm, estimated from pearls used in this study (see bead sizes and diameter measurements in table 1) as well as verification measurements on a cross section of a low-quality pearl.



Figure 5. The steps involved in the process of harvesting Australian akoya pearls. A: Bivalves are removed from their cages. B: The separator cleans the pearls from the tissues. C: Separated pearls are collected by opening a valve at the bottom of the machine. D: Wooden revolving drums are used to wash the pearls in a saltwater solution. E: A selection of the day's harvest with the range of colors displayed at the front. Photos by Laura Otter.

This is high compared to Japanese akoya, whose nacre thickness averages only 0.2 mm in the northern islands and rarely exceeds 0.3 mm in the warmer waters of the southern islands (Strack, 2006).

The pearls are harvested in the austral winter months of June and July. Following the Japanese akoya culturing tradition, pearl oysters at Broken Bay Pearls are generally not seeded a second time but are

removed from their cages (figure 5A) and sacrificed by cutting through the adductor muscle. A motorized separator (figure 5B) reduces the soft tissues to small pieces while the relatively heavy pearls collect at the bottom of the machine and are extracted by opening a valve (figure 5C). Adhesive organic remains are removed by using a suspension of salt in freshwater (figure 5D), while walnut shells are used to buff the pearls, a common practice in Japan. The pearls are spread out on cloth for air drying in sunlight (figure 5E), which could be understood as a minimal *maeshori*¹ luster enhancement, depending on how strictly this is defined. However, it is emphasized here that no color- or luster-improving substances or processes are otherwise applied—e.g., dyes, bleaches, or alcohol, which are traditionally used for Japanese akoya (Gervis and Sims, 1992). After drying, the pearls are graded for quality, color, luster, shape, and size.

Figure 6. This silver pendant features a round 7.5 mm silver akoya pearl from Broken Bay. The silver disk is etched with a pattern resembling the reflection of the moon on the rippling ocean. Photo courtesy of AngelRock Jewellers.



Figure 7. Naturally white cultured pearls from Broken Bay: two necklaces, a pair of stud earrings, and three loose pearls. Photo courtesy of Percy Marks Jewellers.

The farm in Broken Bay produces several thousand pearls per year, and about 50% are of gem quality. The average size ranges from 6.5 to 8 mm and in very rare cases up to 10 mm. Keshi pearls also occur as a result of the seeding process, as the fragile epithelial cells of the mantle tissue can be injured or separated and develop into small pearl sacs that produce an additional though unintended small pearl (Hänni, 2006). Broken Bay pearls are cultured in a wide range of colors. Bodycolors include the traditional akoya silver and white (figures 6 and 7, respectively), though light and dark yellows appear almost as frequently and blues are also occasionally seen (again, see figure 1). Intense orange bodycolors (as in BBP05 and BBP06, table 1) occur very rarely. Overtones range from orange, pink, silver, white, silver-green, and cream through yellow to gold.

The two seeders at Broken Bay have noticed a difference in the respective proportions of silver to white, yellow, and blue bodycolors they produced (figure 8). After tracing back and comparing their in-

¹*Maeshori* treatment aims to enhance a pearl's luster. This can involve different chemical (e.g., alcohol or salty solutions) or physical (e.g., heating and cooling) treatments. It is traditionally applied to Japanese akoya cultured pearls, often in combination with dyes or bleaches.

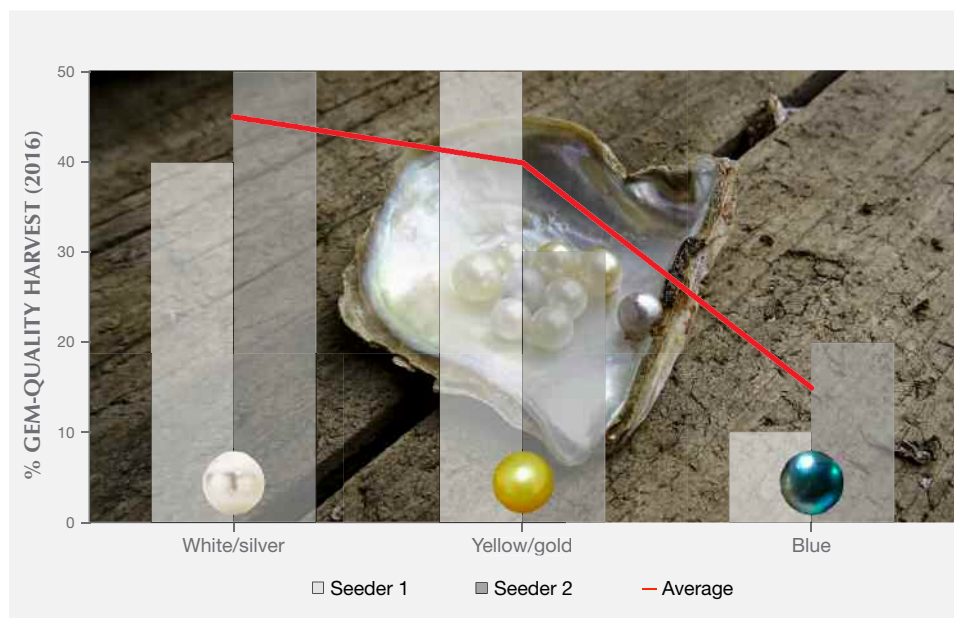


Figure 8. Broken Bay's two seeders tag their own cages of freshly seeded bivalves to track the proportions of bodycolors produced. The proportion of white, yellow, and blue bodycolors is seen to vary between the seeders, and this is attributed to slight variations in the selection of appropriate tissue graft. The red line shows the overall abundance of each bodycolor as an average of both seeders. Photo by Laura Otter.

dividually seeded bivalves, which had been color coded on their cages, the seeders concluded that while cutting and preparing the tissue grafts, they each favored slightly different colored tissue pieces, thus influencing the harvested colors.

It is understood that modern pearl farming yields many positive consequences for the local ecosystem. The exceptionally high filtering capabilities of the *Pinctada* species, up to 25 liters per gram of dried tissue each day, effectively remove heavy metals, organic pollutants, and nutrient overloads from coastal environments (Gifford et al., 2004). Hence, pearl farming reduces turbidity and eutrophication—i.e., the excess supply of nutrients coupled with high biomass loads. Turbidity is reduced by the long-line systems, with their many large cages that act as a barrier for near-surface currents. Eutrophication is reduced by the high filter-feeding capacities of the bivalves. Furthermore, the timber-free long-line systems prevent entanglement of dolphins and other marine species. Following these environmentally friendly principles, Broken Bay Pearls has been successful in supplying a wide range of Australian wholesalers and jewelers each year.

MATERIALS AND METHODS

The lead author attended Broken Bay's annual pearl harvest in June 2016 to obtain pearls for this study. The mollusks were brought to the farm by boat and taken from the nets and opened by hand. After extraction from the separator, the pearls were spread out on a cloth and examined. The author visually determined a wide range of bodycolors, including yel-

low, silver, white, cream, orange, blue, and light silver-green of various shades and intensities (again, see figure 5E). A total of 14 saltwater cultured pearls were selected as representative of each bodycolor group for the present study. The pearls were found to be mostly round (samples BBP01 to BBP13) to semi-round (BBP14) in shape. They measured 6.7–8.2 mm in diameter with an average of 7.2 mm, while their weight varied from 2.0 to 3.7 ct (table 1).

Raman spectra of each pearl were collected at room temperature using a Horiba Jobin Yvon LabRAM HR Evolution confocal spectrometer with 473 nm laser excitation. All Raman spectra were recorded in the 100–2000 cm^{-1} range using a spectral acquisition time of 12 seconds and four accumulations. A grating with 1800 grooves/mm was used with a slit width of 100 μm to ensure a high spectral resolution of approximately 0.8 cm^{-1} . PL spectra were collected using the same instrument, although measurement conditions were adjusted to a spectral acquisition time of eight seconds and five accumulations per cycle, with 532 nm excitation wavelength. Data were collected in the 537–710 nm range using a grating with 600 grooves/mm to achieve higher intensities at a spectral resolution of approximately 2 cm^{-1} .

Mid-FTIR spectra were recorded with a Thermo Scientific Nicolet iN10 infrared microscope using a 149 \times 149 μm aperture and an acquisition time of five seconds per spectrum. All data were collected with 16 scans per spectrum in the range of 675–3970 cm^{-1} using a liquid-nitrogen-cooled MCT-A detector sys-

tem and a spectral resolution of 4 cm^{-1} . A background spectrum was collected in air before each sample spectrum. Raman, PL, and FTIR data were collected at Macquarie University's Department of Earth and Planetary Sciences in Sydney.

UV-Vis spectra were recorded 16 times per sample in the 380–800 nm range using a Leica Orthoplan microscope in combination with a Leica MPV-SP UV-Vis spectrophotometer at Johannes Gutenberg University in Mainz, Germany. Microscope-based UV-Vis data acquisition is generally performed without the use of an integrated sphere accessory, which made it necessary to collect all spectra in specular reflection mode with well-defined incident and reflected light angles (2° in this study). Specular reflection mode uses a thin plate of polished aluminum as reference material, since it has higher reflectance properties than BaSO_4 or Spectralon, which are only used when data collection is performed in diffuse reflection mode. All spectra were collected using $32\times$ magnification by focusing on the surface of each pearl. Some individual samples (namely BBP05, BBP07, BBP11, and BBP12) yielded reflectance values greater than 100%, which made it necessary to focus slightly subsurface.

RESULTS AND DISCUSSION

Raman Spectrometry. Figure 9 presents seven representative Raman spectra of Australian akoya cultured pearls across the range of bodycolors as outlined in table 1 (yellow, orange, silver, white, green, and blue). The most prominent peaks are assigned to aragonite (black lines), the crystalline calcium carbonate polymorph generally associated with lustrous pearls of the *Pteriidae* family (e.g., Jacob et al., 2011; Wehrmeister et al., 2011; Hänni, 2012). Among these, the highest-intensity band was observed at 1085 cm^{-1} , as well as a doublet with peak centers at 701 and 705 cm^{-1} , which are assigned to ν_1 (symmetric stretching) and ν_4 (in-plane bending) modes of the carbonate anion (CO_3^{2-}) in aragonite (e.g., Urmos et al., 1991). The small peak at 1462 cm^{-1} is identified as ν_3 (in-plane asymmetric stretching); due to its low intensity, this peak is not observed equally well in all pearls. In addition, aragonite lattice modes were observed between 170 and 300 cm^{-1} (Urmos et al., 1991). All pearls showed virtually identical peak centers, intensities, and backgrounds except for the darkest one (BBP11), which had a slightly increased background (again, see figure 9). This is due to a stronger contribution of luminescence in the background signal, pos-

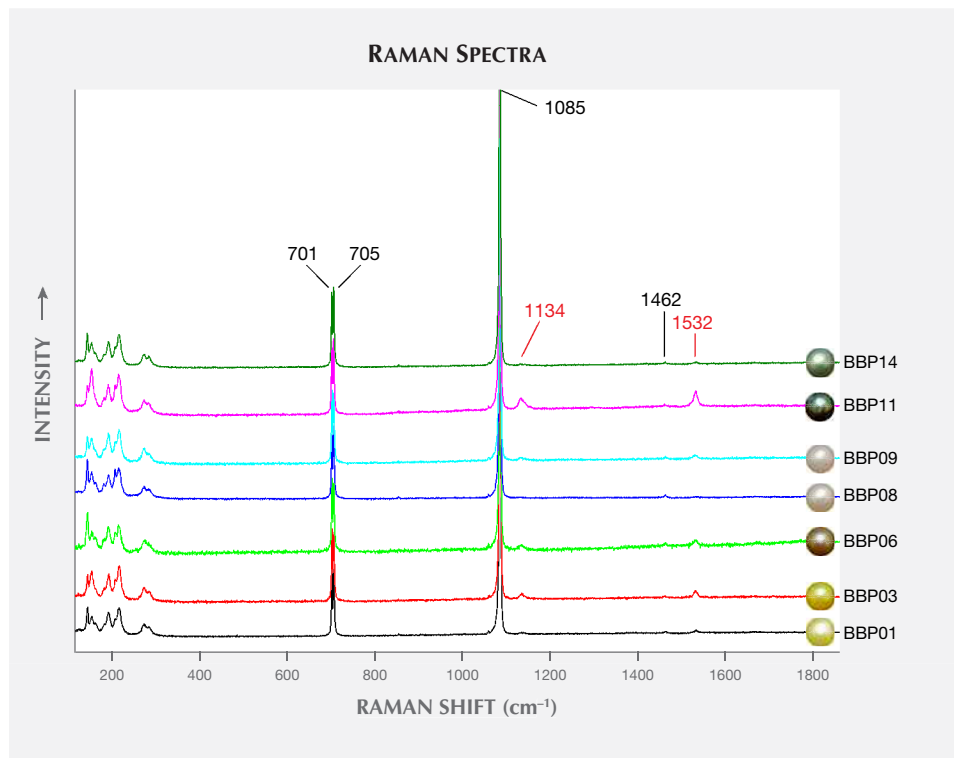


Figure 9. Raman spectra of seven Broken Bay akoya cultured pearls from *Pinctada imbricata fucata* normalized to the highest-intensity peak at 1085 cm^{-1} and offset for clarity. The selection shows a cross section of bodycolors ranging from light yellow (BBP01, BBP03), orange (BBP06), white (BBP08), silver (BBP09), and dark blue (BBP11) to green (BBP14). The spectra show identical bands for aragonite (black lines), while two remaining peaks are attributed to pigments (red lines).

sibly related to pigments contributing to the pearl's dark blue color.

Peaks of weaker intensity (figure 9, red lines) corresponded to distinct bands of pigments (polyenes) consistent with previously published values (e.g., Karampelas et al., 2007; Soldati et al., 2008; Karampelas et al., 2009; Bersani and Lottici, 2010). These include peaks at 1134 and 1532 cm^{-1} that belong to the stretching modes of the C-C single bond (ν_2) and C=C double bond (ν_1) in the polyene chain biomolecule, respectively. Samples with darker bodycolors such as dark blue (BBP11), orange (BBP06), and dark yellow (BBP03) displayed the highest intensities for both pigment-related peaks, while green (BBP14), white (BBP09), and light yellow and yellow (BBP01) pearls exhibited much lower intensities. For the white specimen BBP08, the peaks were undetectable.

Photoluminescence Spectrometry. All PL spectra showed virtually identical features in the yellow to red region at 585, 610, 625, and 685 nm (figure 10). Sharp peaks in the spectra resulted from the Raman effect and occurred independently of the PL bands. These included features in the 538–540 nm region (vibrational properties of the aragonite lattice modes),

as well as discrete peaks, caused by vibrational modes of the carbonate ion, at 552 nm (in-plane bending, ν_4), 565 nm (symmetric stretching, ν_1), 577 nm (in-plane asymmetric stretching, ν_3), and 630 nm (caused by $\nu_1 + \nu_3$; Xu and Poduska, 2014). The four PL bands had positions similar to those previously published for cultured pearls from *Pinctada maxima*, *Pinctada margaritifera*, *Pinctada mazatlanica*, and *Pteria sterna*, at 620, 650, and 680 nm; however, the weak band at 585 nm has not been described for these species (Miyoshi et al., 1987; Kiefert et al., 2004; Karampelas et al., 2011; Karampelas, 2012). It should be noted that all bands appear less defined for the akoya pearls than for those produced by *Pinctada maxima*, *Pinctada margaritifera*, and *Pteria sterna*. PL features in pearls are generally thought to result from organic compounds within the nacre composite material (Karampelas et al., 2007). This is consistent with our observation that the relative PL intensity correlated with color intensity in the specimens and stronger pigment-related Raman bands (figure 9).

Mid-FTIR Spectrometry. The most prominent features observed in the spectra of cultured pearls from Australian *Pinctada imbricata fucata* were caused by the

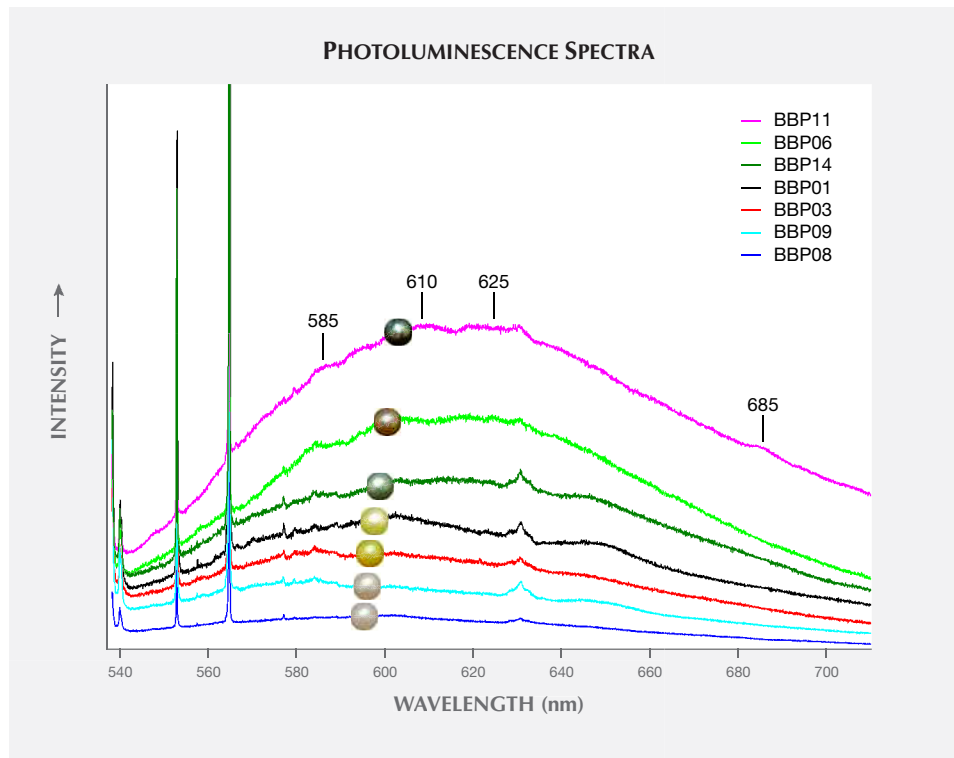


Figure 10. Uncorrected photoluminescence (PL) spectra of the seven akoya cultured pearls whose Raman spectra are shown in figure 9. Spectra are offset for clarity while maintaining their original order of relative PL intensities. All spectra show identical features at 585, 610, 625, and 685 nm, with varying amounts of luminescence that correlate with the color intensity of the samples. Peaks in the 538–540 nm region as well as at 552, 565, 577, and 630 nm originate from the Raman effect of aragonite.

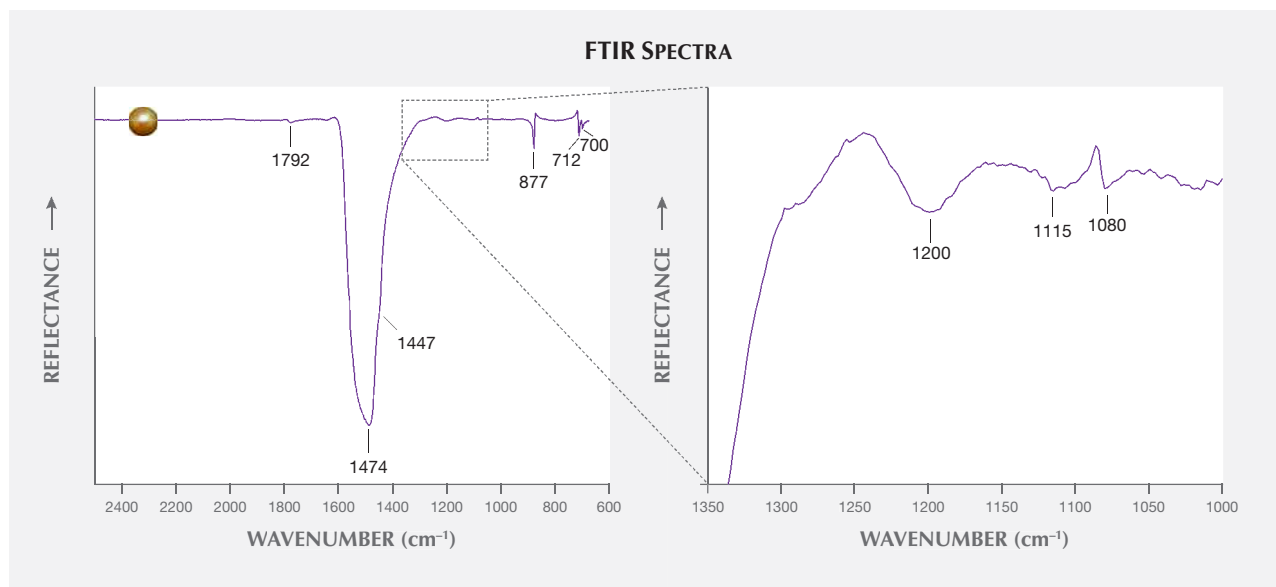


Figure 11. Left: The mid-FTIR spectrum of an orange sample from Broken Bay Pearls (BBP05) shows bands at 700, 712, 877, 1447, 1474, and 1792 cm^{-1} that are characteristic for aragonite and were found in all other samples. However, this sample also shows several weak peaks in the 1000–1350 cm^{-1} region (red box in A). Right: Enlargement of this region reveals several small peaks at around 1200 and 1115 cm^{-1} that are assigned to sulfate and polysaccharide groups of the organic component. The weak band at 1080 cm^{-1} results from stretching vibrations of the carbonate.

intrinsic vibrational modes of the aragonite crystal lattice (figure 11, left), namely ν_{4b} and ν_{4a} at 700 and 712 cm^{-1} (internal modes), ν_2 at 877 cm^{-1} (out-of-plane bending mode), and ν_3 at 1447 cm^{-1} (in-plane asymmetric stretching). Strong absorption bands in the 1600–1400 cm^{-1} range resulted from several closely spaced peaks at 1570, 1525, 1488, 1474, and 1440 cm^{-1} (Andersen and Brecevic, 1991; Xu and Poduska, 2014). The highest-intensity band at 1474 cm^{-1} was previously found to result from a combination of the lattice mode peaks at 220, 263, 290, and 700 cm^{-1} (Andersen and Brecevic, 1991; Xu and Poduska, 2014). A weak band at 1792 cm^{-1} was caused by a combination of the ν_1 and ν_{4a} modes, while ν_1 (symmetric stretching vibration) was observed in figure 11, right (an enlargement of the red box in figure 11, left). Three other bands in figure 11 (right) can be attributed to different organic compounds in nacre: Broad bands at around 1200 and 1115 cm^{-1} likely resulted from S-O of sulfate and C-O of polysaccharide groups, respectively (Marxen et al., 1998). The peak at 1080 cm^{-1} is assigned to the symmetric stretching vibration (ν_1) of CO_3^{2-} .

UV-Vis Spectrometry. The pearls were grouped into different UV-Vis spectra with similar characteristics. For better readability, overlapping spectra were offset by adding or subtracting each measured intensity

value with a fixed offset value expressed as a percentage relative to the original measured intensity (figure 12). The specimens shown in figure 12A consist of two pearls of a rather cooler shade of yellow, which might result from green hues and/or overtones (BBP01 and BBP03), plus silver (BBP10) and green (BBP14) samples. They are characterized by a slight spectral trough in the blue-green to yellow region between 450 and 600 nm (except for BBP01) and have a sharp drop in relative intensity from approximately 645 nm onward. The light yellow specimen BBP01 (table 1) has the brightest bodycolor, which correlates with the highest relative intensity. Of the two pearls in figure 12B, one has a light silver bodycolor with a blue hue and overtone (BBP07) and the other a dark blue (BBP11) bodycolor with green, blue, and silver hues and overtones (hues and overtones determined by visual observation). The spectrum of the dark blue pearl (BBP11) shows two distinct troughs at 425–530 nm (blue to green region) and 550–625 nm (green to orange region), while the silver specimen (BBP07) has a trough at 425–625 nm. Both pearls display a sharp drop in reflectance at 625 nm. A lower intensity over the full spectral range is responsible for the dark color of BBP11; specimen BBP07 shows a similar pattern, but at an overall higher relative intensity that corresponds to its brighter color. Figure 12C shows spectra

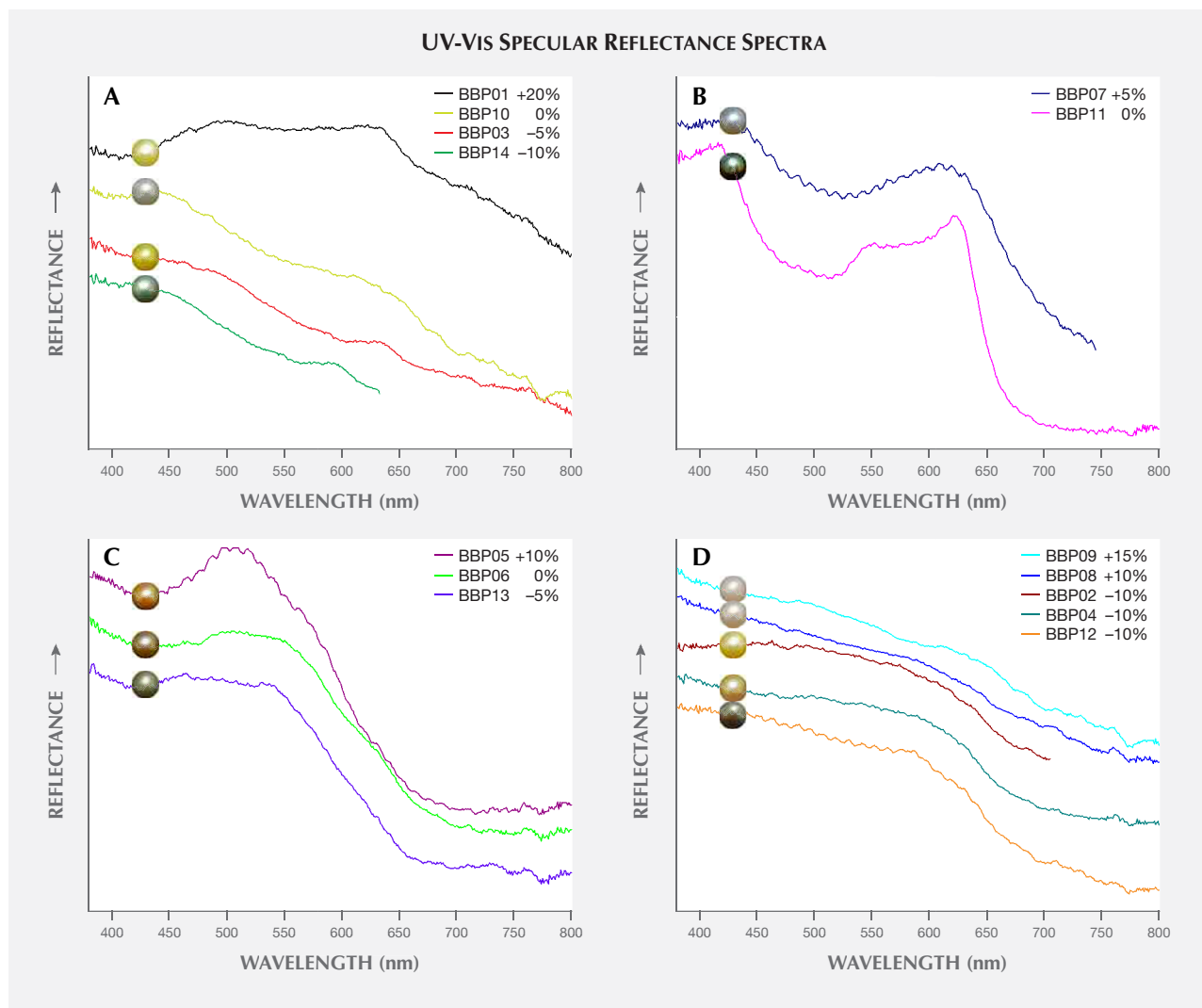


Figure 12. UV-Vis specular reflectance spectra of 14 Australian akoya samples normalized to the reflectance yield of a polished aluminum plate. Some spectra are offset for clarity, with offset values provided in the legends.

for the pearls with orange bodycolor (BBP05 and BBP06) as well as for a green specimen with warm pink and silver hues and overtones (BBP13). These specimens exhibit distinct absorption features between 400 and 475 nm and between 600 and 800 nm that correspond to the blue region and the orange to red region, respectively. At 800 nm, relative intensities drop to below 55%. Lastly, figure 12D shows spectra for pearls that exhibit white (BBP08 and BBP09), dark silver (BBP12), and yellow bodycolors (BBP02 and BBP04). Note that the pearls with yellow bodycolor from figure 12D have orange and golden hues and overtones, while the other yellow specimens in figure 12A show green and yellow hues and overtones. Their spectra lack distinct absorption features and differ only in relative intensity.

Altogether, each pearl's bodycolor is strongly dependent on its specific absorption features and relative intensities, which are produced by different combinations of pigments present in the organic compound of the nacre (Soldati et al., 2008; Karampelas et al., 2009; Karampelas, 2012). The bodycolor was found to correlate with the overall relative intensity of the PL spectra (figure 10), where the dark blue specimen (BBP11) exhibited the highest relative PL intensity, while the yellow, white, and silver samples had the lowest.

Although the pearls from this study show a wide variety of spectral features, they can be differentiated from untreated pearls of some other species: Gray, yellow, and black pearls from *Pinctada margaritifera* as well as gray, yellow, and green pearls from *Pinc-*

tada mazatlanica show a distinct trough at 700 nm that is not present in any of the akoya pearls from this study. In those pearls, the feature is associated with the presence of pigments (Miyoshi et al., 1987; Elen, 2002; Karampelas et al., 2011; Cartier et al., 2012). Further, dark gray pearls from both *Pinctada margaritifera* and *Pinctada mazatlanica* show an absorption feature at 405 nm that is known to result from uroporphyrin pigments (Homkrajae, 2016, and reference therein). Yellow pearls from *Pinctada maxima* show a broad trough from 310 to 510 nm, with individual absorption features centered at 360 and 430 nm. This distinguishes them from the *Pinctada imbricata fucata* pearls from this study, which also show various absorption features at higher and lower wavelengths (table 2). While discrimination between naturally colored pearls across different saltwater species appears promising, naturally colored white akoya pearls remain indistinguishable from untreated white pearls produced by other mollusks, due to the absence of characteristic spectral features. Also, the discrimination of naturally colored akoya cultured pearls produced in eastern Australia from others of different

geographic origin is considered beyond the capability of this method.

CONCLUSIONS

We have presented a description and characterization of akoya cultured pearls from the Central Coast region of New South Wales in eastern Australia. Apart from the absence of bleaching or dyeing procedures, the pearls are cultured following the Japanese tradition. Their natural variety of bodycolors ranges from lighter and darker golden yellows to different shades and intensities of orange and blue to the classic silver and white. These colorful akoya pearls can be used to create modern, nature-inspired jewelry (see figures 1 and 6) as well as classic pieces (figure 7).

Raman and FTIR spectroscopy verified the main mineral phase as aragonite (figures 9 and 11), and pigment-related Raman bands were observed at 1135 and 1530 cm^{-1} . These belong to stretching modes of the C-C single bond and C=C double bond of the polyene chain biomolecules. These peaks were found to have the highest intensities for samples with darker bodycolors, such as dark blue, orange, and yellow.

TABLE 2. Summary of color and corresponding absorption centers of untreated cultured pearls from *P. fucata*, *P. margaritifera*, and *P. maxima*.

Mollusk species	Pearl bodycolor	Absorption centers in specific range (nm)				References
		350–450	450–550	550–650	650–800	
<i>P. imbricata fucata</i>	Silver	None	None	~550 ^a	775	This study
	Yellow (cool hue and overtone)	None	None	~550 ^a	c.a. ^b	
	Yellow (warm hue and overtone)	None	None	None	c.a.	
	White	None	None	None	c.a.	
	Orange	430	None	None	~720 ^a	
	Green	~430 ^a	None	~550 ^a	~720 ^a	
	Silver with strong blue overtone	None	513	None	c.a.	
<i>P. margaritifera</i>	Dark blue	None	510	580	~750 ^a	
<i>P. margaritifera</i>	White and silver	None	None	None	None	Elen (2002)
	Gray	None	460, 495	None	700	Karampelas (2012)
	Yellow	None	None	None	700	Elen (2002)
	Black	405	495	None	700	
<i>P. maxima</i>	Yellow	360, 430	495	None	None	Elen (2002)
	Gray	None	460, 495	None	None	Karampelas (2012)
<i>P. mazatlanica</i>	Dark gray	405	None	None	700	
	Yellow to green	~358 ^a	~423 ^a	None	700	Homkrajae (2016)
	White and silver	None	None	None	None	

^aApproximate peak center due to a very broad or indistinct feature

^bc.a. = continuous absorption

low (figure 9, red lines). The pearls showed four rather indistinct PL bands in the yellow to red region of the electromagnetic spectrum (figure 10), which were similar to the band positions observed for *Pinctada maxima*, *Pinctada margaritifera*, *Pinctada mazatlanica*, and *Pteria sterna* bivalves (though not as prominent). FTIR spectroscopy of an intense orange pearl revealed the presence of sulfates and polysaccharides representative of organic compounds (figure 11). Lastly, UV-Vis specular reflectance spec-

troscopy showed several absorption features in the visible range that result from the pearls' different bodycolors, hues, and overtones (figure 12, A–D). This technique was found to be useful in discriminating between diverse colorful akoya pearls from this study and cultured pearls from *Pinctada margaritifera*, *Pinctada mazatlanica*, and *Pinctada maxima* bivalves (table 2), while akoya pearls from other locations as well as white specimens from various species are likely not distinguishable.

ABOUT THE AUTHORS

Ms. Otter (laura.otter@hdr.mq.edu.au) and Mr. Agbaje are PhD candidates at the Macquarie University Department of Earth and Planetary Sciences in Sydney. Dr. Huong is postdoctoral researcher at the Institute of Earth Sciences, Karl Franzens University in Graz, Austria. Dr. Häger is a scientist at the Centre for Gemstone Research at Johannes Gutenberg University in Mainz, Germany, and lectures at the Gemstone and Jewelry Design Department at the University for Applied Sciences in Idar-Oberstein. Dr. Jacob is professor of earth sciences and biomineralization at Macquarie University.

ACKNOWLEDGMENTS

We gratefully acknowledge Ian and Rose Crisp as well as Peter Clift from Broken Bay Pearls Pty Ltd for the opportunity to visit their pearl farm during seeding and harvest season, and for providing all the pearls shown in this study and answering all our

questions. Dr. Jennifer Rowland is kindly thanked for skillful editing of the final manuscript. We thank Ursula Wehrmeister, Dilmi Herath, Michael Förster, Christoph Lenz, and Matthew A. Kosnik for many enriching discussions. Dr. Wayne O'Connor, center director for aquaculture at the Port Stephens Fisheries Centre, NSW Department of Primary Industries, is kindly acknowledged for insightful comments on an earlier draft. Furthermore, we thank Celeste Boonaerts from AngelRock Jewellers, Cameron Marks from Percy Marks Jewellers, and Wayne O'Connor for providing photographs. This work is part of the lead author's PhD thesis; she is supported by an Australian Government International Postgraduate Research Scholarship (IPRS). Mr. Agbaje is supported by a Macquarie University Research Excellence Scholarship, and Dr. Jacob is financially supported by the Australian Research Council via a Future Fellowship and a Discovery Grant. Lastly, we thank three anonymous reviewers for providing very constructive and valuable comments.

REFERENCES

- Acosta-Salmón H., Martínez-Fernández E., Southgate P.C. (2005) Use of relaxants to obtain saibo tissue from the blacklip pearl oyster (*Pinctada margaritifera*) and the Akoya pearl oyster (*Pinctada fucata*). *Aquaculture*, Vol. 246, No. 1-4, pp. 167–172, <http://dx.doi.org/10.1016/j.aquaculture.2004.12.010>
- Andersen F.A., Brecevic L. (1991) Infrared spectra of amorphous and crystalline calcium carbonate. *Acta Chemica Scandinavica*, Vol. 45, No. 10, pp. 1018–1024, <http://dx.doi.org/10.3891/acta.chem.scand.45-1018>
- Bersani D., Lottici P.P. (2010) Applications of Raman spectroscopy to gemology. *Analytical and Bioanalytical Chemistry*, Vol. 397, No. 7, pp. 2631–2646, <https://doi.org/10.1007/s00216-010-3700-1>
- Cartier L.E., Krzemnicki M.S., Ito M. (2012) Cultured pearl farming and production in the Federated States of Micronesia. *G&G*, Vol. 48, No. 2, pp. 108–122, <http://dx.doi.org/10.5741/GEMS.48.2.108>
- Elen S. (2002) Identification of yellow cultured pearls from the black-lipped oyster *Pinctada margaritifera*. *G&G*, Vol. 38, No. 1, pp. 66–72, <http://dx.doi.org/10.5741/GEMS.38.1.66>
- Gervis M.H., Sims N.A. (1992) *The Biology and Culture of Pearl Oysters (Bivalvia: Pteriidae)*. Overseas Development Administration of the United Kingdom (London) and International Center for Living Aquatic Resources Management (Manila).
- Gifford S., Dunstan R.H., O'Connor W., Roberts T., Toia R. (2004) Pearl aquaculture—profitable environmental remediation? *Science of the Total Environment*, Vol. 319, No. 1-3, pp. 27–37, [http://dx.doi.org/10.1016/S0048-9697\(03\)00437-6](http://dx.doi.org/10.1016/S0048-9697(03)00437-6)
- Gilbert P.U., Bergmann K.D., Myers C.E., Marcus M.A., DeVol R.T., Sun C.-Y., Blonsky A.Z., Tamre E., Zhao J., Karan E.A., Tamura N., Lemer S., Giuffre A.J., Giribet G., Eiler J.M., Knoll A.H. (2017) Nacre tablet thickness records formation temperature in modern and fossil shells. *Earth and Planetary Science Letters*, Vol. 460, pp. 281–292, <https://doi.org/10.1016/j.epsl.2016.11.012>
- Hänni H.A. (2006) A short review of the use of 'keshi' as a term to describe pearls. *Journal of Gemmology*, Vol. 30, No. 1/2, pp. 52–58 <http://dx.doi.org/10.15506/JoG.2006.30.1.51>
- (2007) A description of pearl farming with *Pinctada maxima* in South East Asia. *Journal of Gemmology*, Vol. 30, No.

- 7/8, pp. 357–365, <http://dx.doi.org/10.15506/JoG.2007.30.7.357>
- (2012) Natural pearls and cultured pearls: a basic concept and its variations. *The Australian Gemmologist*, Vol. 24, No. 11, pp. 256–266.
- Homkrajae A. (2016) Gem News International: Spectral characteristics of *Pinctada mazatlanica* and *Pinctada margaritifera* pearl oyster species. *G&G*, Vol. 52, No. 2, pp. 207–208.
- Jacob D.E., Wirth R., Soldati A.L., Wehrmeister U., Schreiber A. (2011) Amorphous calcium carbonate in the shells of adult *Unionoida*. *Journal of Structural Biology*, Vol. 173, No. 2, pp. 241–249, <https://doi.org/10.1016/j.jsb.2010.09.011>
- Karampelas S. (2012) Spectral characteristics of natural-color saltwater cultured pearls from *Pinctada maxima*. *G&G*, Vol. 48, No. 3, pp. 193–197, <http://dx.doi.org/10.5741/GEMS.48.3.193>
- Karampelas S., Fritsch E., Mevellec J.-Y., Gauthier J.-P., Sklavounos S., Soldatos T. (2007) Determination by Raman scattering of the nature of pigments in cultured freshwater pearls from the mollusk *Hyriopsis cumingi*. *Journal of Raman Spectroscopy*, Vol. 38, No. 2, pp. 217–230, <http://dx.doi.org/10.1002/jrs.1626>
- Karampelas S., Fritsch E., Mevellec J.-Y., Sklavounos S., Soldatos T. (2009) Role of polyenes in the coloration of cultured freshwater pearls. *European Journal of Mineralogy*, Vol. 21, No. 1, pp. 85–97, <http://dx.doi.org/10.1127/0935-1221/2009/0021-1897>
- Karampelas S., Fritsch E., Hainschwang T., Gauthier J.-P. (2011) Spectral differentiation of natural-color saltwater cultured pearls from *Pinctada margaritifera* and *Pteria sterna*. *G&G*, Vol. 47, No. 2, p. 117.
- Kiefert L., Moreno D.M., Arizmendi E., Hänni H.A., Elen S. (2004) Cultured pearls from the Gulf of California, Mexico. *G&G*, Vol. 40, No. 1, pp. 26–39, <http://dx.doi.org/10.5741/GEMS.40.1.26>
- Kripa V., Mohamed K.S., Appukuttan K.K., Velayudhan T.S. (2007) Production of Akoya pearls from the Southwest coast of India. *Aquaculture*, Vol. 262, No. 2–4, pp. 347–354, <https://doi.org/10.1016/j.aquaculture.2006.09.047>
- Marxen J.C., Hammer M., Gehrke T., Becker W. (1998) Carbohydrates of the organic shell matrix and the shell-forming tissue of the snail *Biomphalaria glabrata* (Say). *The Biological Bulletin*, Vol. 194, No. 2, pp. 231–240, <http://dx.doi.org/10.2307/1543052>
- Miyoshi T., Matsuda Y., Komatsu H. (1987) Fluorescence from pearls to distinguish mother oysters used in pearl culture. *Japanese Journal of Applied Physics*, Vol. 26, Part 1, No. 4, pp. 578–581, <http://dx.doi.org/10.1143/JJAP.26.578>
- O'Connor W.A., Lawler N.F., Heasman M.P. (2003) Trial farming the akoya pearl oyster, *Pinctada imbricata*, in Port Stephens, NSW: Final Report to Australian Radiata Pty Ltd., pp. 1440–3544.
- Otter L.M., Wehrmeister U., Enzmann F., Wolf M., Jacob D.E. (2014) A look inside a remarkably large beaded South Sea cultured pearl. *G&G*, Vol. 50, No. 1, pp. 58–62, <http://dx.doi.org/10.5741/GEMS.50.1.58>
- Scarratt K., Bracher P., Bracher M., Attawi A., Safar A., Saeseaw S., Homkrajae A., Sturman N. (2012) Natural pearls from Australian *Pinctada maxima*. *G&G*, Vol. 48, No. 4, pp. 236–261, <http://dx.doi.org/10.5741/GEMS.48.4.236>
- Soldati A.L., Jacob D.E., Wehrmeister U., Häger T., Hofmeister W. (2008) Micro-Raman spectroscopy of pigments contained in different calcium carbonate polymorphs from freshwater cultured pearls. *Journal of Raman Spectroscopy*, Vol. 39, No. 4, pp. 525–536, <http://dx.doi.org/10.1002/jrs.1873>
- Strack E. (2006) *Pearls*. Rühle-Diebener, Stuttgart, Germany.
- Urmos J., Sharma S.K., Mackenzie F.T. (1991) Characterization of some biogenic carbonates with Raman spectroscopy. *American Mineralogist*, Vol. 76, No. 3–4, pp. 641–646.
- Wehrmeister U., Jacob D.E., Soldati A.L., Loges N., Häger T., Hofmeister W. (2011) Amorphous, nanocrystalline and crystalline calcium carbonates in biological materials. *Journal of Raman Spectroscopy*, Vol. 42, No. 5, pp. 926–935, <http://dx.doi.org/10.1002/jrs.2835>
- Xu B., Poduska K.M. (2014) Linking crystal structure with temperature-sensitive vibrational modes in calcium carbonate minerals. *Physical Chemistry Chemical Physics*, Vol. 16, No. 33, pp. 17634–17639, <http://dx.doi.org/10.1039/C4CP01772B>

For online access to all issues of GEMS & GEMOLOGY from 1934 to the present, visit:

gia.edu/gems-gemology

